LETTER

Dynamics extracted from fixed cells reveal feedback linking cell growth to cell cycle

Ran Kafri[1]*, Jason Levy[2]*, Miriam B. Ginzberg[1], Seungeun Oh[1], Galit Lahav[1] & Marc W. Kirschner[1]

Biologists have long been concerned about what constrains variation in cell size, but progress in this field has been slow and stymied by experimental limitations[1]. Here we describe a new method, ergodic rate analysis (ERA), that uses single-cell measurements of fixed steady-state populations to accurately infer the rates of molecular events, including rates of cell growth. ERA exploits the fact that the number of cells in a particular state is related to the average transit time through that state[2]. With this method, it is possible to calculate full time trajectories of any feature that can be labelled in fixed cells, for example levels of phosphoproteins or total cellular mass. Using ERA we find evidence for a size-discriminatory process at the G1/S transition that acts to decrease cell-to-cell size variation.

Size is an obvious and distinguishing feature of cells, characteristic of their physiology and pathology. A barrier to studying size control in mammalian cells is the inaccuracy in measuring size, growth rate, and the dynamics of pathways controlling growth and proliferation[1]. To overcome these obstacles we developed ERA, a procedure for extracting dynamics and regulatory relationships from a single image of a population of individual fixed cells. ERA makes use of the fact that, at steady state, the number of cells in any particular molecular state is related to the rate at which cells transit through that state[2]. Using this method, we calculated the dynamics of cell growth and cell cycle progression and investigated the processes that limit size variation.

To determine precise cell cycle dynamics from a single image of fixed cells, we considered the fact that unsynchronized proliferating cells are often found to be in a quasi-steady state, in which the proportion of cells in each phase of the cell cycle is stable (Fig. 1). We determine cell cycle position by measuring the levels of both DNA and a fluorescent reporter of the geminin degron (mAG-hGem)[3]. In the context of the present study, mAG-hGem serves as a marker for the activity of the anaphase-promoting complex (APC) in its active APC[Cdh1] form (hereafter termed APC for simplicity). The scatter plot in Fig. 1a demonstrates the well-known decrease in APC activity in late G1 (resulting in mAG-hGem accumulation), which is followed by doubling of DNA in S phase. Reactivation of APC at mitosis results in a sharp fall in mAG-hGem fluorescence followed by cytokinesis, during which DNA levels drop by one half (Fig. 1). For populations
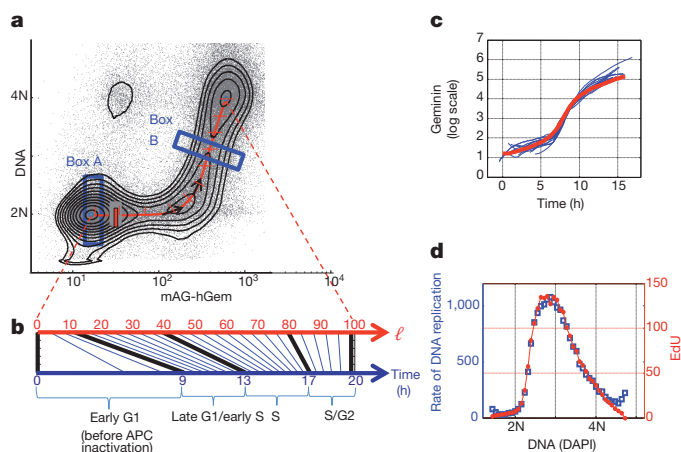

Figure 1 | Dynamic information from static data using ERA. a, Levels of DNA (DAPI) and geminin (mAG-hGem) in an unsynchronized, exponential population of HeLa cells. The black contour lines denote the distribution, f, of cells within the DNA/geminin plane. Also shown is the average cell cycle trajectory, ℓ (red). The different densities of cells in boxes A and B result from the different rates at which cells traverse those regions. **b**, The transformation of the cell cycle axis, ℓ, to a real-time axis. For convenience we chose 100 units of ℓ to represent a complete path from the beginning of G1 to the end of G2. **c**, **d**, Comparison of ERA with direct dynamical measurements. Accumulation of mAG-hGem was followed in ten individual live cells by time-lapse microscopy (blue lines) and compared to the dynamics of mAG-hGem calculated from fixed cells using ERA (red) (**c**). DNA-replication rate was measured by exposing cells to a 20-min pulse of EdU before fixation. Average levels of EdU fluorescence per cell (indicating rate of DNA replication) are plotted (blue) as a function of DAPI, giving a measure of the mean rate of DNA replication as a function of passage through S. For comparison, ERA was used to calculate DNA-replication rates directly from fixed cells not treated with EdU (red). N denotes number of chromosome sets.

BOX 1

The ERA balance equation

ERA rests on the fact that at steady state the difference, $-n_t \nabla \cdot (fv)$, between the rates at which cells enter and leave any given molecular state must be balanced by the increase in cell count in that state. n_t is the total number of cells in the population at time t, f is the proportion of cells in the given state (indicated by the black contour lines in Fig. 1a), and v is the rate at which cells pass through that state. As f does not change with time, the number of cells at any given state as a function of time is $fn_t = fn_0 e^{\alpha t}$. These considerations result in a simple balance equation:

$$-\nabla \cdot (fv) + B = \alpha f \qquad (1)$$

in which α is the proportion of cells dividing per unit time and B is a term accounting for cell division (see Supplementary Materials). As we will show, equation (1) can be used to derive accurate time profiles from a single measurement on a population of fixed cells. If more parameters are measured, the dimensionality of the plot increases but the analyses remain the same.

Equation (1) is free of any mechanistic assumptions or free variables and is grounded only on a basic conservation principle akin to conservation of mass. Equation (1) and its implementations throughout this study are based on two main assumptions outlined in detail in the Supplementary Materials: (1) the representation axes (which in the present study are DNA and APC activity) appropriately represent both individual and collective cell behaviour; and (2) the steady-state assumptions described above apply.

[1]Department of Systems Biology, Harvard Medical School, Boston, Massachusetts 02115, USA. [2]Department of Mathematics and Statistics, University of Ottawa, Ottawa, Ontario K1N 6N5, Canada.
*These authors contributed equally to this work.

12 h after fixation that have not reached confluence, the distribution, *f*, of cells in the plane defined by these two measurements is independent of the time at which cells were sampled and fixed, as shown in Supplementary Materials. The existence of a stationary-state condition imposes a quantitative relationship between the proportion of cells in different regions of the plot and the rates of molecular events (that is, changes in DNA and APC activity). For example, in Fig. 1, because every cycling cell passes through the labelled regions A and B, the higher cell count in region A must mean that cells traverse this region at slower rates than in region B (see Box 1).

Our goal in this study was to use equation (1) (Box 1) to determine the growth rate of cells at different points in the cell cycle; in other words to solve for *v*. To solve equation (1) we reduced the number of dimensions from DNA (first dimension) and APC activity (second dimension) to a single dimension, ℓ, representing cell cycle progression over time (see Box 2). Although ℓ is not directly measured, it can be calculated from *f*, which is obtained experimentally (see Supplementary Materials). Figure 1a shows ℓ (red curve) superimposed on the single-cell measurements.

Figure 1c compares mAG-hGem dynamics of live cells obtained from time-lapse microscopy to dynamics of fixed cells calculated by ERA. There is near-perfect agreement. To further demonstrate the utility of ERA, we compared the rate of DNA replication obtained by labelling live cells with 5-ethynyl-2′-deoxyuridine (EdU) to the rate of DNA replication obtained by ERA of 4′,6-diamidino-2-phenylindole (DAPI)-stain intensity in fixed cells (Fig. 1d). As with the previous example, we obtained a considerable overlap between the measurements. Both examples show that ERA calculations can resolve dynamics to a timescale on the order of minutes.

To characterize cell-growth dynamics during the cell cycle we quantified the protein mass of individual cells by measuring the total fluorescence intensity from cells stained with a succinimidyl ester dye (Alexa Fluor 647 succinimidyl ester; SE-A647), which covalently reacts
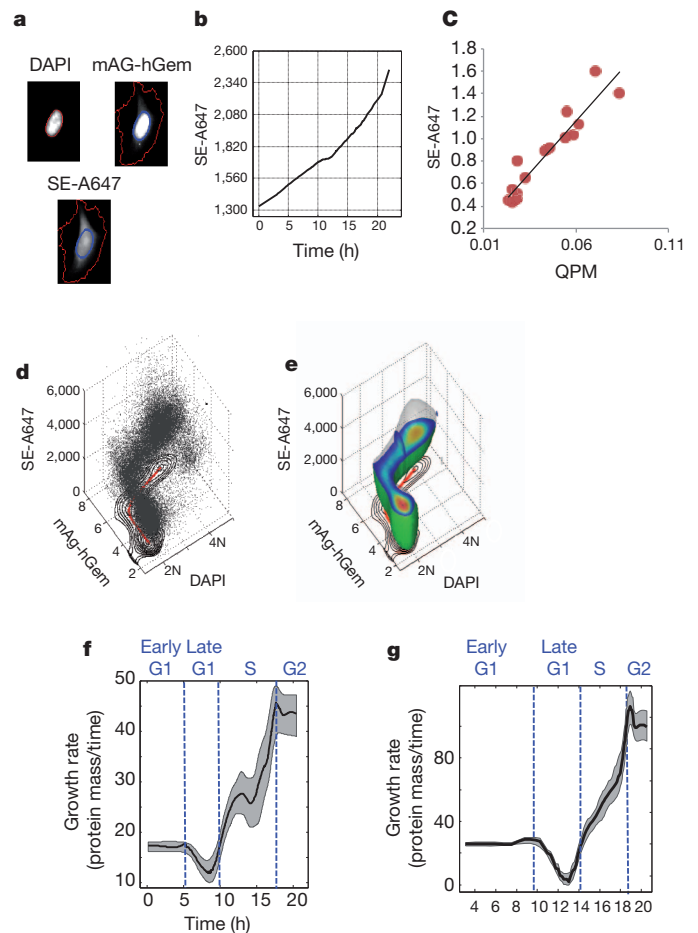
Figure 2 | Calculation of growth as a function of cell cycle progression using ERA. a, Cells were stained and imaged for DNA content (DAPI), the geminin degron (mAG-hGem) and for protein content (SE-A647). **b**, Growth during cell cycle progression, computed by ERA. **c**, Comparison of SE-A647 fluorescence intensity with quantitative phase microscopy measurements in single cells. Each data point represents a single cell measured for both protein content (SE-A647) and phase retardation (QPM). **d**, A scatter plot for the levels of DNA (DAPI), geminin (mAG-hGem) and cell size (SE-A647) in an unsynchronized population of HeLa cells. Also shown is the projection of the two-dimensional distribution of geminin and DNA overlaid with ℓ. **e**, The three-dimensional probability distribution from the data shown in **d**. **f, g**, Growth rate versus time for HeLa cells (**f**) and retinal pigment epithelial (RPE1) cells (**g**) calculated by ERA. Confidence intervals (grey) of ±1 standard error are shown as described in Supplementary Materials.

Reducing the dimensionality of equation (1)

Confining equation (1) to the cell cycle trajectory, ℓ, and integrating results in an expression (equation (2)) that relates measured probability density, *f*, to the rate of progression through the cell cycle, ω, we have:

$$\omega(\ell) = \alpha \frac{2 - F(\ell)}{f(\ell)} \quad (2)$$

in which $F(\ell) = \int_1^\ell f(\ell) d\ell$. Furthermore, because $\omega(\ell) \equiv \frac{d\ell}{dt}$, we can use results of equation (2) to calculate a complete time axis for the dynamics of the measured processes using:

$$t(\ell_0) = \int_{\ell=1}^{\ell_0} \frac{1}{\omega} d\ell \quad (3)$$

in which $t(\ell_0)$ is the time it takes for a cell starting at position $\ell = 1$ (G1) to reach position ℓ_0 on the cell cycle axis, ℓ. As shown in Fig. 1, equations (1)–(3) transform a single, non-temporal measurement on fixed cells into temporal trajectories represented on time axis, *t*. Figure 1b shows the nonlinear transformation (the ERA transform) of a path, ℓ, defined by molecular events, onto a time axis. We conveniently chose 100 units of ℓ to represent a complete path from G1 to G2. We do not include M (metaphase) in this analysis because the number of cells in M is very small. Real time enters this calculation through the doubling time of the population, $\tau = \frac{\log(2)}{\alpha}$. For solutions of ERA in more than two dimensions see Supplementary Materials.

---

with lysyl groups. This is a good measure of protein mass[4] and correlates well with physical measurements of dry mass by quantitative phase microscopy (QPM), which has accuracy of better than 1%[5] (Fig. 2c). From these measurements, we assembled a three-dimensional single-cell data set simultaneously reporting cell size and cell cycle stage for millions of fixed cells (Fig. 2a, d, e). As expected, our data show an approximate doubling in protein fluorescence in a single cell cycle (Fig. 2b).

For four very different cell lines, the growth in mass during the cell cycle, as calculated by ERA, produced very similar trajectories that are neither linear nor exponential (Fig. 2f, g and Supplementary Materials). The results show that growth rates increase with progression through the cell cycle and reach a maximum during G2, consistent with a recent study using QPM[6]. What was previously unknown is a transient slowdown in protein-accumulation rate at the G1/S transition in all cell lines (Fig. 2f, g). Because this slowdown occurs for a relatively short time, it is not surprising that it was not detected in previous time-course measurements on synchronized populations. Further, by aligning cells using

molecular markers of cell cycle progression rather than time, ERA avoids the clouding effects of imperfect synchronization. Plots of growth rate as a function of mass are similar to those obtained recently with the suspended microchannel resonator[7] (Supplementary Materials).

The existence of stable and narrow distributions of cell size suggests cell-autonomous feedbacks controlling size variability. To search for such feedbacks we calculated the joint dependency of growth rate, v, on size, s, and cell cycle position, ℓ (Fig. 3). The size distribution within any interval along the cell cycle path ℓ, $\Delta_\ell = (\ell - w, \ell + w)$, is governed exclusively by (Fig. 3a): (1) the size distribution of cells entering the interval from the previous cell cycle stage; (2) the size distribution of cells leaving the interval into a later cell cycle stage; and (3) cell growth within the interval. Such a formulation allows the construction of a three-term balance equation relating growth rate to cell size within the interval (see Box 3).

Figure 3b plots how v depends on s at three different points in the cell cycle; late G1 ($\ell = 20$), the G1/S transition ($\ell = 40$) and late S phase ($\ell = 80$). A notable result of this analysis is the shift to a negative slope of growth rate versus cell size for cells around the G1/S transition (see slope for $\ell = 40$). This negative slope is unexpected as it suggests that at this point small cells have higher growth rates than larger cells. This
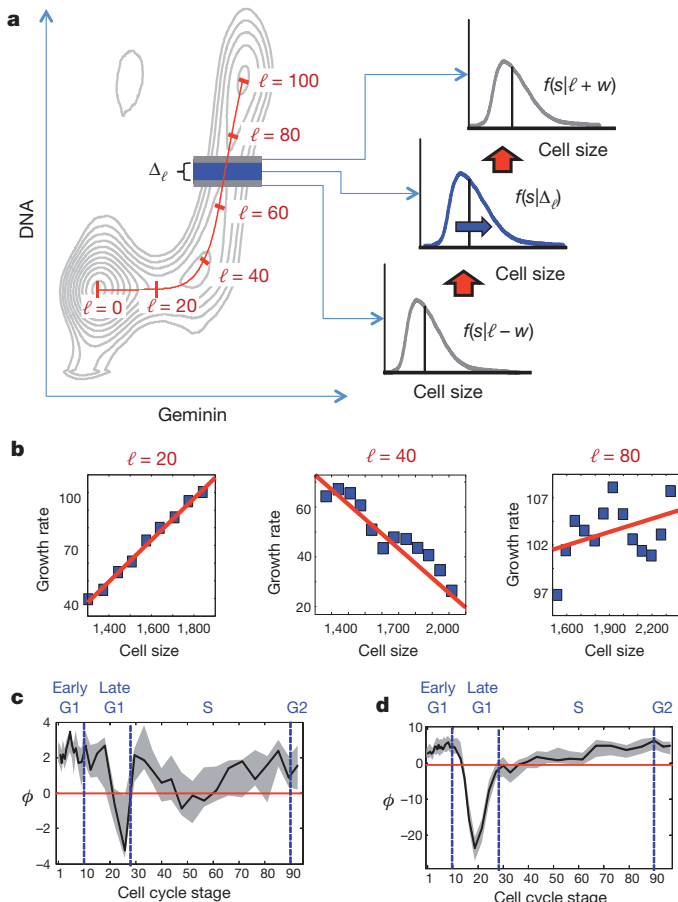
Figure 3 | Rate of cell growth as a function of size and cell cycle. Size discrimination at the G1/S transition. **a**, Calculation of growth rate as a function of size for a defined interval, Δ_ℓ, on the cell cycle axis, ℓ. To calculate feedback regulation as a function of cell size, the size distributions of cells entering and leaving Δ_ℓ are estimated from the sizes of cells on the boundary of Δ_ℓ. **b**, Plots of growth rate versus cell size at late G1 ($\ell = 20$), the G1/S transition ($\ell = 40$) and late S phase ($\ell = 80$). **c, d**, The slope, ϕ, of growth rate versus cell size plotted as a function of ℓ, for HeLa cells (**c**) and RPE1 cells (**d**). The red horizontal line positioned at $\phi = 0$ is added to emphasize the distinction between positive and negative slopes (positive and negative feedbacks). Blue vertical lines demarcate borders between different stages of cell cycle. Confidence intervals (grey): 90% in **c**; ± 1 standard deviation in **d**.

BOX 3

Analysing growth as a function of size

To obtain the size distributions of cells entering and leaving a given interval we consider the size distributions of cells positioned at the borders of that interval (Fig. 3a). These distributions are formally approximated by the conditional probability distributions, $F(s|\ell - w)$ and $F(s|\ell + w)$, in which $F(s|\ell - w)$ is the cumulative probability distribution of cell size, s, among cells in the state $\ell - w$ at the entrance to the interval $\Delta_\ell = (\ell - w, \ell + w)$ (marked red in Supplementary Fig. 13), and similarly with $F(s|\ell + w)$. The width, $\Delta \ell = 2w$, represents the resolution limit of the calculation. Using this construction we obtain an equation for the rate of cell growth as a function of cell size and cell cycle position:

$$v(s, \Delta_\ell) = \alpha \frac{(2 - \lambda_A)F(s|\ell - w) - (2 - \lambda_A - \lambda_B)F(s|\ell + w) - F(s|\Delta_\ell)\lambda_B}{f(s|\Delta_\ell)\lambda_B} \quad (4)$$

in which $F(s|\Delta_\ell) = F(s|(\ell - w, \ell + w))$ is the size distribution within the interval Δ_ℓ, λ_A is the fraction of cells occupying all cell cycle stages preceding Δ_ℓ, and λ_B is the fraction of cells in Δ_ℓ. We use the notations F and f to refer to cumulative and non-cumulative probability distributions, respectively. To further evaluate how the growth-rate/cell-size dependency relates to cell cycle progression, we translate ℓ along the cell cycle axis and repeatedly solve equation (4) for all points on ℓ.

cell-size-dependent growth rate implies a negative feedback linking growth rate to cell size, effectively constraining cell-to-cell size variability in the population.

Figure 3c, d shows the slope, ϕ, of the growth rate versus cell size as a function of the cell cycle progression axis, ℓ. A positive ϕ implies that larger cells have higher growth rates than smaller cells, whereas a negative ϕ implies the opposite. $\phi = 0$ indicates that growth is independent of cell size. Calculating ϕ for four different cell lines (Fig. 3c, d and Supplementary Materials) yields feedback spectra that consistently acquire negative values at the G1/S transition.

The strict interpretation that cell size negatively feeds back on growth rate at G1/S depends on the assumption that progression along ℓ is independent of cell size (see Supplementary Materials). This is not the only possibility. An alternative interpretation is that size variation is limited not by repressing the growth rate of large cells but by inhibiting the rate at which small cells progress along the cell cycle. Whichever of these interpretations is correct, equation (4) identifies fingerprints of a cell-size discriminatory process, occurring at the G1/S transition, that distinguishes small and large cells and results in an increase in the homogeneity of cell size in the proliferating population. These results support very early findings suggesting cell-size regulation at the G1/S transition[8].

To test further whether growth at G1/S is different for large and small cells, we treated HeLa cells for 1 h with a proteasome inhibitor (MG132), a translation inhibitor (cycloheximide), or an mTOR inhibitor (rapamycin). If growth rates and cell cycle progression were independent of cell size, both large and small cells would be equally affected by any treatment. Our results show that MG132 increased the variation in the size of cells at G1/S. (Fig. 4b). Cycloheximide had the opposite effect (Fig. 4c). mTOR inhibition also decreased cell-to-cell size variability, but to a lesser extent than cycloheximide (Fig. 4d). These results indicate that the decrease in cell-size variance is at least partially driven by a cell-size discriminating proteasome activity. The possibility that size variation is further controlled by size-dependent translation activity seems less likely in light of the decreased size variation following cycloheximide treatment.

Proliferating cells in an unsynchronized population are distributed among different molecular states (that is, cell cycle stages). In situations in which this distribution does not change with time and in which
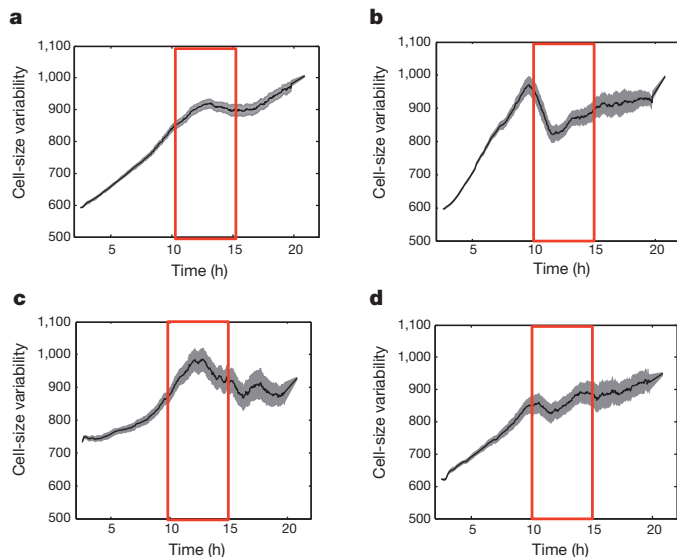
Figure 4 | Effects of drug treatments on size variability at G1 exit. Cell-size variability (full width/half maximum) as a function of cell cycle time for HeLa cells incubated for 1 h with 0.001 v/v dimethylsulphoxide (**a**), 1 μM cycloheximide (**b**), 10 μM MG132 (**c**) and 100 nM rapamycin (**d**). Confidence intervals are shown in grey.

individual cells shift from state to state in a defined sequence, it is possible to calculate dynamical features from simple static single-cell measurements[9,10], which may be obtained from microscopy or flow cytometry. We have shown that both our primary measurements and the functions derived from them are time invariant (see Supplementary Materials), thereby meeting these criteria. Others[11] previously suggested that data from fixed cells could, in principle, be used to extract dynamic information; we have now provided an explicit mathematical framework to make this analysis possible. Using ERA we show that cell-to-cell size variation is regulated by a negative feedback at the G1/S transition. We can also use ERA to characterize other dynamic processes that cannot in general be measured in real time in living cells, such as the temporal changes in phosphoproteins during the cell cycle (Supplementary Materials).

METHODS SUMMARY

Reagents, cells and antibodies are described in Supplementary Information. Cells were plated and fixed at 10^5 cells per ml in 15-cm dishes. They were fixed in paraformaldehyde, permeabilized and stained with 0.04 μg ml^{-1} succinimidyl-ester-linked Alexa dyes diluted in DMSO (Alexa Fluor 647 carboxylic acid, succinimidyl ester; Invitrogen; A-20106). Slides were imaged with a Nikon Ti Inverted Fluorescence Microscope with Perfect Focus controlled by Nikon Elements software. We used the scan-slide function to image the full area of the slide at ×20 magnification. Image analysis was performed with custom-written software (EnsembleThresher). The details of the software and the calculation of the ERA parameters are discussed in detail in Supplementary Information.

1. Mitchison, J. M. Growth during the cell cycle. *Int. Rev. Cytol.* **226,** 165–258 (2003).
2. Deen, W. M. *Analysis of Transport Phenomena* 2nd edn (Oxford University Press, 2012).
3. Sakaue-Sawano, A. *et al.* Visualizing spatiotemporal dynamics of multicellular cell-cycle progression. *Cell* **132,** 487–498 (2008).
4. Mitchison, J. M. *The Biology of the Cell Cycle* 128 (University Press, 1971).
5. Popescu, G. *et al.* Optical imaging of cell mass and growth dynamics. *Am. J. Physiol. Cell Physiol.* **295,** C538–C544 (2008).
6. Mir, M. *et al.* Optical measurement of cycle-dependent cell growth. *Proc. Natl Acad. Sci. USA* **108,** 13124–13129 (2011).
7. Son, S. *et al.* Direct observation of mammalian cell growth and size regulation. *Nature Methods* **9,** 910–912 (2012).
8. Killander, D. & Zetterberg, A. A quantitative cytochemical investigation of the relationship between cell mass and initiation of DNA synthesis in mouse fibroblasts *in vitro. Exp. Cell Res.* **40,** 12–20 (1965).
9. Hendrix, R. W. & Zwaan, J. Cell shape regulation and cell cycle in embryonic lens cells. *Nature* **247,** 145–147 (1974).
10. Tzur, A., Kafri, R., LeBleu, V. S., Lahav, G. & Kirschner, M. W. Cell growth and size homeostasis in proliferating animal cells. *Science* **325,** 167–171 (2009).
11. Jacobberger, J. W., Avva, J., Sreenath, S. N., Weis, M. C. & Stefan, T. Dynamic epitope expression from static cytometry data: principles and reproducibility. *PLoS ONE* **7,** e30870 (2012).

Author Contributions R.K. and J.L. developed the method (ERA) for extracting dynamic information and calculating feedback spectra from fixed populations, designed algorithms, wrote all image-processing software and analysed data. R.K. designed all experiments and wrote the manuscript. J.L. contributed significantly to all conceptual challenges and to writing the manuscript. M.B.G. contributed conceptually on levels of the study, made many important measurements and calculations and contributed to the writing of the manuscript. S.O. provided interferometry-derived cell mass measurements. G.L. and M.W.K. contributed to the formulation of the problem, development of the ideas and the writing of the manuscript.

Author Information Reprints and permissions information is available at www.nature.com/reprints. The authors declare no competing financial interests. Readers are welcome to comment on the online version of the paper. Correspondence and requests for materials should be addressed to M.W.K. (marc@hms.harvard.edu).